



Grain Boundary Sliding In Experimental Deformation Of Octachloropropane

Jin-Han Ree

Department of Earth and Environmental Sciences, Korea University

Anam-dong 5-1, Seongbuk-ku, Seoul 136-701, Korea

reejh@kuccnx.korea.ac.kr,

Table of contents

[Abstract](#)

[1. Introduction](#)

[2. Grain Boundary Sliding](#)

[3. Accommodation Mechanisms for Grain Boundary Sliding](#)

[4. Experimental Examples](#)

[5. Evolution and Implications of Grain Boundary Sliding](#)

[6. Recognition of Grain Boundary Sliding](#)

[7. References](#)

[Previous Section](#) [Home](#) [Next Section](#)

Abstract

Grain boundary sliding is an important deformation process not only in diffusion creep but also in dislocation creep. The details of grain boundary sliding and associated accommodation mechanisms are discussed in experimentally deformed octachloropropane at a high homologous temperature. Grains unsuitably oriented for basal slip tend to deform by grain boundary sliding. Grain boundary sliding is accommodated mainly by grain boundary diffusion and intracrystalline plastic deformation. With grain boundary sliding, openings develop preferentially along grain boundaries at a low angle to the shortening direction, maintaining a steady openings ratio of 0.5–3% of the sample volume without the development of any large-scale fracture. The preferred orientation of remnants of grain boundary openings is the best evidence of grain boundary sliding.

[Previous Section](#) [Home](#) [Next Section](#)

1. Introduction

In plastic flow of polycrystalline materials above about 30 - 50% of their absolute melting temperature, deformation mechanisms divide into two groups, lattice mechanisms and boundary mechanisms, based on whether the individual processes are independent of, or dependent on, the presence of grain boundaries (Langdon, 1975, 1981; Langdon and Vastava, 1982). With lattice mechanisms, deformation occurs by processes taking place within the grains. These mechanisms are possible in both polycrystalline materials and single crystals. With boundary mechanisms, deformation occurs by processes associated with the presence of grain boundaries. These mechanisms are possible only in polycrystalline materials (Langdon, 1975). Grain boundary sliding and diffusional creep are two major processes of boundary mechanisms. Although it is usually difficult to find clear microstructural evidence for grain boundary sliding and diffusional creep in naturally or experimentally deformed rocks (Schmid et al., 1977; Schmid, 1982; Behrmann, 1985), it has been suggested that grain boundary sliding can be the dominant deformation mechanism in some cases, particularly in fine-grained mylonites or ultramylonites (e.g. Behrmann, 1985; Behrmann and Mainprice, 1987; Stünitz and Fitz Gerald, 1993; Fliervoet et al., 1997).

In this paper, grain boundary sliding and associated accommodation mechanisms will be reviewed with some clear examples from *in-situ* deformation of an organic analog material. The recognition of grain boundary sliding in naturally deformed rocks will also be discussed. Most of the contents and experimental examples in this paper were already published by Ree (1994). The major addition of this chapter is the time-lapse movies of the experimental examples from Ree (1994).

[Previous Section](#) [Home](#) [Next Section](#)

2. Grain Boundary Sliding

Grain boundary sliding is a process in which grains slide past each other along, or in a zone immediately adjacent to, their common boundary (Langdon and Vastava 1982). Adams and Murray (1962) first observed grain boundary sliding in experimentally deformed bicrystals of NaCl and MgO, where offset of scratch marker lines pre-inscribed across the grain boundary occurred. *In-situ* observation of grain boundary sliding in a Zn-Al alloy was made by Naziri et al. (1973, 1975), using electron microscopy. They inferred grain boundary sliding from the observation of grain neighbor switching during deformation. Considering the extensive grain boundary migration in their photographs, however, neighbor switching alone does not provide convincing evidence of grain boundary sliding, because neighbor switching can be achieved by grain boundary migration only (Means and Ree, 1990; Bons and Urai, 1992).

Grain boundary sliding is a probable process in plastic flow of polycrystals if there is deformation incompatibility among grains and if the necessary accommodation mechanisms for grain boundary sliding can operate (see below). Figure 1(a) shows, in a schematic way, three possible situations for grain boundary sliding, where there is a strain jump, rotation jump, or translation jump between grains. However strain, rotation or translation jumps do not necessarily produce grain boundary sliding, if material at the contact or boundary can maintain coherent contact by suitably matching deformation of the two grains (Fig. 1b, see also Means and Jessell 1986).

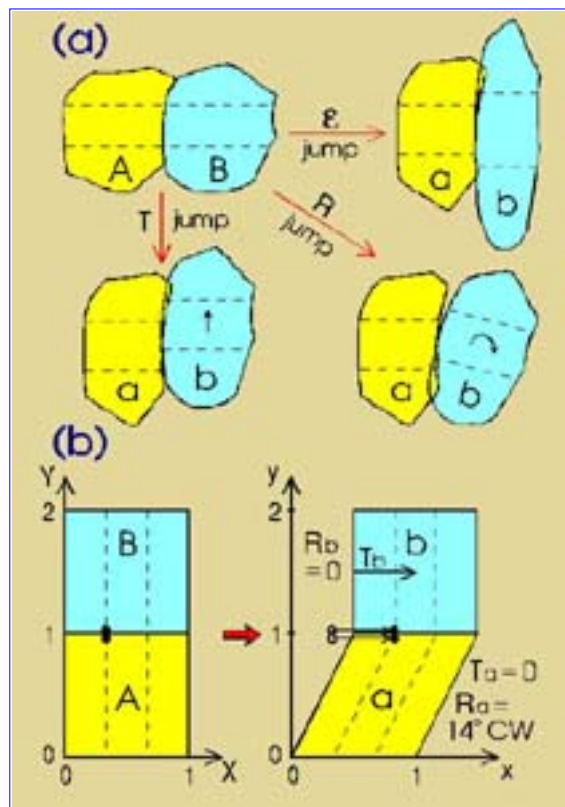


Fig. 1. (a) Schematic diagram illustrating why grain boundary sliding occurs. Top left: two grains (A & B) in the undeformed state with two straight marker lines (broken lines). Top right: grain boundary sliding due to a strain jump. Bottom right: grain boundary sliding due to a rotation jump. Bottom left: grain boundary sliding due to a translation jump. (b) Schematic diagram to show that strain, rotation or translation jumps do not necessarily cause grain boundary sliding. Grain A is dextrally sheared (shear strain = 0.5) while grain B is rigidly translated, inducing a strain jump (from a maximum principal strain of about 0.28 to zero strain), a rotation jump (from about 14° CW rotation of the principal strain direction to zero rotation), and a translation jump (from $T_a = 0$ to $T_b = 0.5$) across the boundary from grain a to b. However, grain boundary sliding does

not occur since material particles at the boundary (black dots) are displaced into the same positions by each domainal deformation of the grains.

Zhang et al. (1994) have shown in a computer modeling of fabric development that the introduction of a small amount of grain boundary sliding sufficiently decreases 'grain interaction' in the intracrystalline plastic deformation regime, and suggested that grain boundary sliding can be a mechanism for accommodating strain incompatibility between neighboring grains. It should be also pointed out that grain boundary sliding has been considered a dominant deformation mechanism in superplasticity, although the term superplasticity does not imply or even define a particular deformation mechanism (Schmid et al., 1977; Poirier, 1985, pp. 204-205; Gilotti and Hull, 1990). For example, there is a general agreement that grain boundary sliding contributes more than 50% of the total strain in superplastic materials (Vastava and Langdon, 1979; Chokshi and Langdon, 1985; Kashyap et al., 1985). This is the case probably when a smaller grain size and/or presence of melt or fluid film along grain boundaries facilitate grain boundary sliding.

[Previous Section](#) [Home](#) [Next Section](#)

3. Accommodation Mechanisms for Grain Boundary Sliding

Some simultaneous accommodation mechanisms must operate to avoid the types of overlaps between sliding grains as shown in Fig. 1, and between a sliding grain and a blocking grain in front of the sliding grain. Many authors have suggested that openings (or voids) also should be avoided to maintain a coherency between grains (e.g. Crossman and Ashby, 1975; Edward and Ashby, 1979). However, complete coherency at grain boundaries is not a rigid requirement in grain boundary sliding (Langdon, 1970). Also grain boundary microcracking can occur even in crystal plastic deformation without a failure (Peach and Spiers, 1996). Therefore we include grain boundary openings in accommodation mechanisms, unless they are connected to make a large-scale fracture (Ree, 1988, 1994). Accommodation mechanisms suggested in the literature of metallurgy and materials science are elastic distortion, dislocation movement and diffusion. The details of grain boundary openings will be explained later.

Elastic distortion can accommodate grain boundary sliding by deforming sliding and blocking grains elastically. With this accommodation mechanism the sliding displacement must be small relative to the length of the sliding surface, and it may be recoverable when the stress is removed (Raj and Ashby, 1971).

Dislocation movement can accommodate grain boundary sliding in such ways as by forming a localized deformation zone adjacent to the triple junction within a blocking grain ("triple-point fold", Fig. 2a) or at ledges of the grain boundary between sliding grains (Gifkins, 1976; Etheridge and Wilkie, 1979; Langdon and Vastava, 1982; Zeuch, 1984; Drury and Humphreys, 1986; Hashimoto et al., 1986), by deforming a whole blocking grain with slip and twinning (Fig. 2b, Crossman and Ashby, 1975), or by climb and glide within the grain boundary mantle (Fig. 2c, Gifkins, 1976).

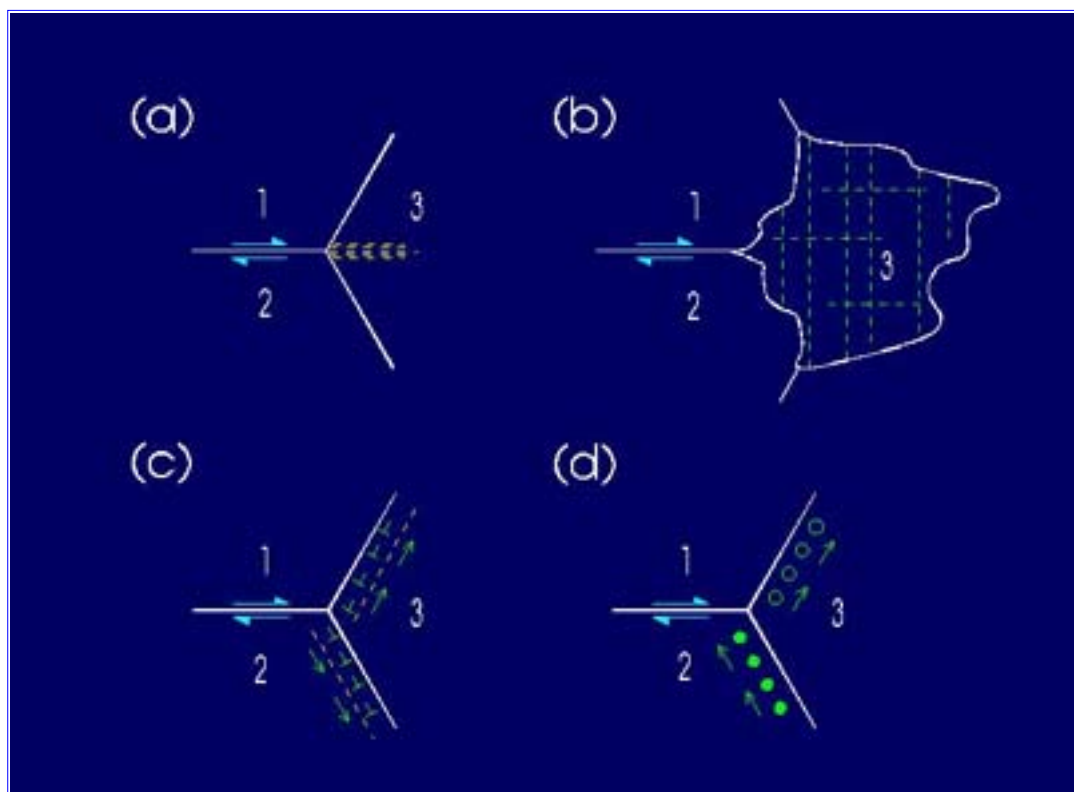


Fig. 2. Accommodation mechanisms of grain boundary sliding. (a) Localized deformation adjacent to the

triple junction within a blocking grain (grain 3). (b) Intragranular plastic deformation of a whole grain. Dotted lines represent deformation bands. (c) Dislocation glide and climb in the grain mantle (after Gifkins 1976). Dotted lines represent boundaries between grain mantle and core. Movements of dislocations in the mantle are schematically shown. (d) Diffusion along grain boundaries around the triple junction (after Gifkins 1976).

Diffusional accommodation occurs by transport of material either along the grain boundaries or through the lattices of grains (Fig. 2d, Raj and Ashby, 1971; Ashby and Verrall, 1973). Grain boundary sliding accommodated by this mechanism is considered as a normal part of diffusional creep, since diffusional creep should be accompanied by grain boundary sliding to maintain coherency between deforming grains (Raj and Ashby, 1971; Ashby and Verrall, 1973; Langdon, 1975; Gifkins, 1976; Speight, 1976; Langdon and Vastava, 1982). However, it will be somewhat arbitrary, like a chicken-and-egg problem, to say that one mechanism accommodates another mechanism in plastic deformation where several coupled deformation mechanisms operate (Jessell personal communication, 1991). To solve this problem, the accommodation can be considered in three ways. First, by comparing the contribution to the total strain, it can be said that the mechanism contributing less strain is the accommodation mechanism. Secondly, if two mechanisms contribute almost the same strain to the total strain, we may treat each deformation mechanism in a time sequence and a mechanism coming later is the accommodation mechanism. Lastly, if the contribution of each mechanism to the total strain is about the same and if the two mechanisms initiate at the same time, then the two mechanisms are mutually accommodating.

[Previous Section](#) [Home](#) [Next Section](#)

4. Experimental Examples

4.1. Experimental Method and Conditions

We deformed thin sheets of octachloropropane (C_3Cl_8 , hereafter called OCP) mixed with marker particles (1000-grit silicon carbide) in a 'Urai press' mounted on the stage of an optical microscope for *in situ* observation and recording of deformation processes. This technique of 'synkinematic microscopy' is explained by Means (1989). Table 1 below shows the experimental conditions. Deformation temperature and strain rate are 60-100° C (75-85% of absolute melting temperature of OCP) and 10^{-5} - 10^{-6} /sec, respectively. OCP under these conditions show mostly crystal-plastic behavior. Other details of sample preparation, experimental conditions, analytical methods and general deformation pictures are given by Ree (1991, 1994).

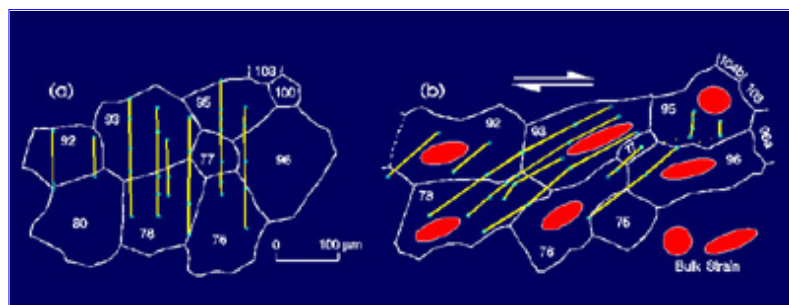
Table 1. Experimental conditions

Experiment	Deformation type	Strain rate* (s^{-1})	Total strain	Temperature (°C)	Duration of deformation (h)
TO-88	Pure shear	2.2×10^{-5}	-0.5 (ϵ_3)	70	6.25
TO-89	Simple shear	7.8×10^{-5}	1.8 (γ)	70	6.42
TO-100	Pure shear	2.3×10^{-5}	-0.5 (ϵ_3)	100	6.17
TO-105	Simple shear	5.3×10^{-5}	1.8 (γ)	80	9.50
TO-110	Simple shear	3.8×10^{-5}	1.3 (γ)	80	9.50
TO-202	Simple shear	9.6×10^{-7}	0.2 (γ)	60	58.00

* Axial strain rate for pure-shear experiments and shear strain rate for simple shear experiments.

4.2. Grain Boundary Sliding by Translation Jump and Accommodation by Diffusion (TO-110)

Figure 3 and its associated movie show grain boundary sliding induced by a translation jump in sample TO-110. In Fig. 3a (bulk shear strain = 0.1), eight material lines were drawn approximately perpendicular to the shear direction with the help of marker particles. After an additional local bulk shear strain of 1.2, all material lines are stretched and rotated (Fig. 3b). All material lines, except two lines passing through grains 95 and 96, remain more or less parallel to each other without any offset. These two lines show offset of about 75 micrometer across the boundary between grains 95 and 96. Grain 95 is not strained much with its basal slip plane is almost perpendicular to the shortening direction. Grain 95 thus is a 'hard' grain with the basal plane unfavorably oriented for slip (Ree 1990). Grain 96 on the other hand is strained almost the same as the bulk strain ellipse for the whole group of grains. Without grain boundary sliding this strain difference should have been represented by a kink-like feature of the material lines without any offset. The offset of the lines running through the two grains implies grain boundary sliding in which grain 95 is translated more or less rigidly over grain 96. All these features can be clearly seen in the movie of Fig. 3.



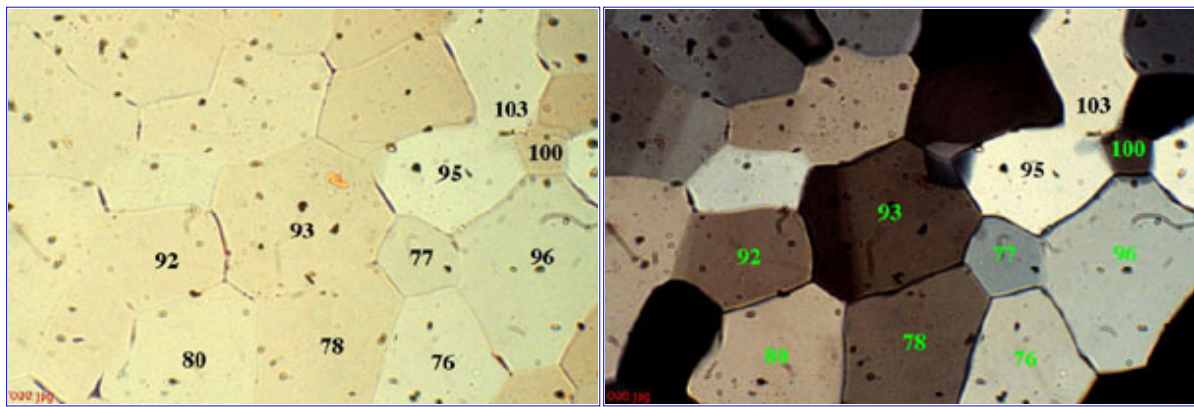


Fig. 3. Maps of the central area of OCP sample TO-110 (a) at bulk shear strain of the whole sample = 0.1 and (b) after deformation (total shear strain = 1.3). Yellow lines represent material lines drawn using marker particles. The bulk strain ellipse (red) of the mapped area is shown in the bottom right of (b). Intragranular strain ellipses are also drawn for most of the grains. (c) Time-lapse movie with plane light and crossed polars from stage (a) to stage (b). Field width of each frame = 0.52 mm. Most small black particles are silicon carbide markers.

At the extensional site associated with the rigid translation of grain 95, the grain boundary sliding is accommodated by diffusional flow. The area occupied by four marker particles across the grain boundary at extensional site increases continuously with the deformation (Fig. 4). The total increase in area is about 50% at the end of the deformation. Diffusional influx of material should account for this area increase. At the compressional site (boundary between grains 95 and 100, Fig. 3a), the exact accommodation mechanism is unclear due to lack of marker particles there.

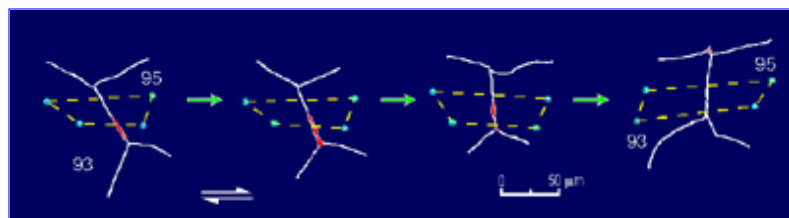


Fig. 4. Evolution of the boundary between grains 93 and 95 in sample TO-110. Grain boundary openings: red. Material lines: yellow. Marker particles are indicated by small circles (light blue).

Grain sliding along the boundary approximately parallel to the bulk shear direction as described above was found at 8 sites in this sample, mainly around hard grains. The amount of offset is usually 70 - 80 micrometer, or 0.6 - 0.7 the average grain diameter. In this sample, however, the contribution of grain boundary sliding to the total strain is minor, accounting for only about 3% (Ree, 1994). Ree (1991, 1994) described the microstructural evolution of this sample in detail.

4.3. Grain Boundary Sliding by Strain and Rotation Jumps (TO-110)

In this example, grain boundary sliding induced by strain and rotation jumps is shown. The strain and rotation jumps result from the difference in initial orientation of the basal slip plane between two grains. It was not possible to identify the accommodation mechanism due to a lack of marker particles.

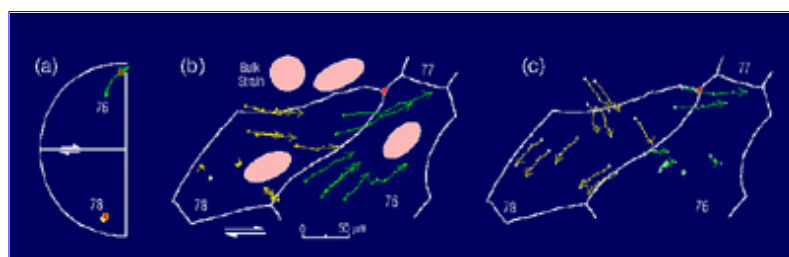


Fig. 5. (a) Western half-circle of a lower hemisphere stereographic projection showing c-axis trajectories of grains 76 and 78 in sample TO-110. Open circle and tip of arrow represent c-axis before and after deformation, respectively. Solid square (red) indicates the c-axis orientation at stage (b). The c-axis of grain 78 remains in almost the same position after the stage of (b). (b) Map of the two grains at a bulk shear strain of 0.7 in the area shown in Fig. 3. Marker particle trajectories (yellow: within grain 78, light green: within grain 76) are drawn using marker particles that remain in the same grain, relative to a fixed particle in grain 78 (solid circle). Initial position of a marker particle is represented by an open circle. The tip of an arrow indicates a marker particle position at a bulk shear strain = 0.7. Particle positions in-between are represented by crosses. (c) Marker particle trajectories at the same stage as in (b) but relative to a fixed particle in grain 76 (solid circle).

Figure 5 shows the c-axis orientations and marker particle trajectories of grains 76 and 78 for a period of deformation during which a bulk shear strain of about 0.7 has accumulated from the stage in Fig. 3(a). The trend of the basal slip plane in grain 76 inclined toward the shear direction at the beginning of the deformation, and its c-axis rotated clockwise by about 25° after an interval of deformation in Fig. 5. On the other hand, the trend of the basal slip plane in grain 78 inclined against the shear direction at the beginning of the deformation and its c-axis stayed in almost the same position (Fig. 5a). The trajectories of marker particles in grain 78 relative to a fixed point within this grain show displacements approximately parallel to the trend of its basal slip plane, suggesting basal slip is the primary deformation mechanism in grain 78 (Fig. 5b). The trajectories of marker particles in grain 76 relative to a fixed point within this grain also tend to show displacements parallel to the trend of its basal plane (Fig. 5c), but whether basal slip predominates or not is unclear because of the rotation of its c-axis. The deformation of these two grains with

different displacement fields results in different maximum stretch (S_1) directions (44° vs. 25° CCW from the shear direction) and in different rotations of S_1 (25° vs. 18° CW), even though the stretch ratios in the two grains (1.9 vs. 2.1) do not differ greatly (Fig. 5b).

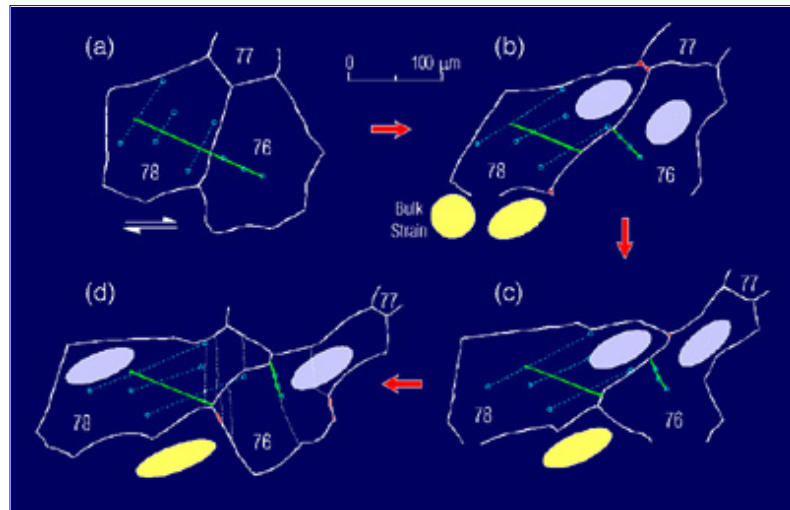


Fig. 6. Offset of a marker line crossing the boundary between grains 76 and 78 in sample TO-110. (a) Bulk shear strain of the sample = 0.1. Additional bulk shear strains of the area in Fig. 3 from the stage (a) are about (b) 0.6, (c) 0.9 and (d) 1.2. Dotted lines (white) in (d) represent subgrain boundaries. The segment of the marker line (thick, light green) in grain 78 was drawn by interpolating the positions of marker particles (light blue, small circle), and the segment in grain 76 was drawn by connecting marker particles. Not all marker particles used to calculate strains are shown.

In Fig. 6(a) a material line was drawn almost perpendicular to the boundary between the two grains using marker particles within the grains. This material line is approximately parallel to the trend of the basal slip plane in grain 78 and at a high angle to that of the basal slip plane in grain 76. As expected with basal slip, the segment of the material line in grain 78 does not change its length and orientation with increasing deformation. If other slip systems had been associated with basal slip, the material line initially parallel to the basal plane should have changed at least its length. On the other hand, the segment of the material line in grain 76 becomes shortened and rotated, producing an offset of the line of about 80 micrometer at the end of the deformation (Fig. 6d). Therefore it is believed that this offset represents grain boundary sliding induced by a strain jump or difference in the maximum stretch direction and a rotation jump between grains 76 and 78.

4.4. Grain Boundary Sliding by Translation Jump and Accommodation by Grain Boundary Opening and Intracrystalline Plasticity (TO-105)

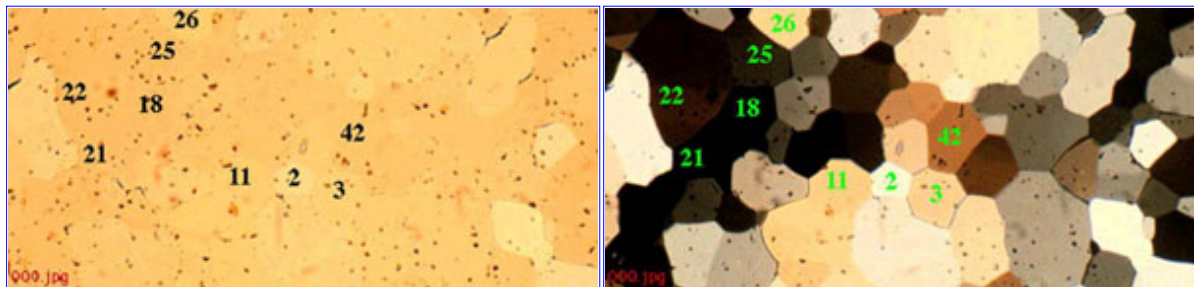


Fig. 7. Time-lapse movies of the deformation of sample TO-105 with plane light (a) and crossed-polars (b). The total shear strain = 1.8. Grain boundary openings begin to occur at shear strain = 1.0. Most small black particles are silicon carbide markers. Dextral shear direction is horizontal. Field width of each frame = 1.46 mm.

Although experimental conditions of TO-105 were almost the same as TO-110 except for the initial c-axis orientation (see below), its deformation behavior was strikingly different from TO-110, with an extensive development of grain boundary openings (Fig. 7) and a greater component of grain boundary sliding in its total deformation. In preparation of an OCP sample before deformation, some preferred orientation of c-axes is always introduced due to the pressing of the sample between two glass slides perpendicular to the plane of observation to obtain a desired sample thickness (30 - 40 micrometer) and some preferred extrusion along the deformation window during sample pressing. The usual shape of c-axis preferred orientation before deformation is a broad, single girdle normal to the direction of shear in simple shearing experiments as in TO-110 and TO-202 (see Fig. 11f). But in sample TO-105 the initial c-axis orientation forms a girdle at a low angle to the shear direction for some unknown reason (Fig. 8a).

Figure 8 shows c-axis fabric diagram before and after deformation, and c-axis reorientation trajectories of some grains in the central area of the sample. During dextral simple shear, the intragranular plastic deformation of grains is accompanied by clockwise rotation of c-axes (Fig. 8c). When the c-axes of most grains are in positions unfavorable for basal slip, grain boundary openings begin to occur in association with relatively rigid translation and rotation of most grains in the sample (Figs. 7 and 8c). Grain boundary openings develop preferentially along boundaries at a low angle to the shortening direction, inclining against the bulk shear direction or the direction of relative displacement of the upper part of the shearing sample. Their widths range from about 2 micrometer up to 40 micrometer with a typical width of about 5 micrometer or about 0.04 the average grain diameter. Their lengths, ranging from about 15 micrometer to 200 micrometer, are mostly 50 micrometer or about 0.4 the average grain diameter. Grain boundary openings grow rapidly during initial stages of deformation to occupy 1 - 2% of the sample area, and remain constant at that value until the deformation stops. Further details of the evolution of these grain boundary openings will be explained later. In

this sample, the contribution of grain boundary sliding to the total strain is about 25% (Ree, 1994).

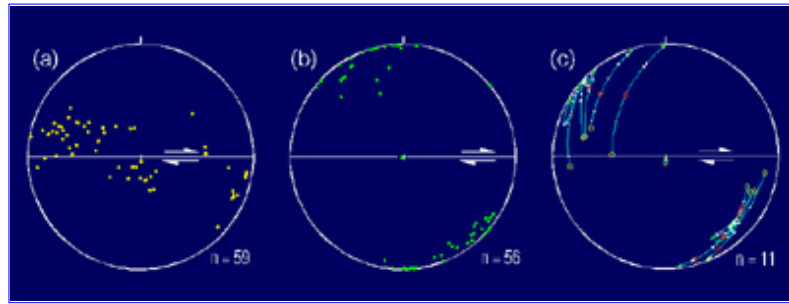


Fig. 8. Lower-hemisphere equal area projections of c-axes of sample TO-105 (a) before and (b) after deformation. (c) c-axis reorientation trajectories. Squares (red) represent c-axis positions when grain boundary openings begin to occur.

An example of grain boundary sliding resulting from translation jump is illustrated in Fig. 9 which shows grain boundary maps, marker particle trajectories and c-axis trajectories for three grains in the sample during an interval of the deformation. The three grains are deformed mainly by intragranular plastic deformation and their c-axes rotate clockwise by 10 - 30° during bulk shear strain of about 0.9 (Figs. 9a and b). As the basal planes of the grains approach an orientation unfavorable for slip, the deformation becomes dominated by grain boundary sliding, and openings begin to develop preferentially along boundaries at a low angle to the shortening direction (Figs. 9c, d, e and f). With an additional shear strain of about 0.4 from the stage of Fig. 9(a), a material line defined by marker particles across the grains 22 and 11 shows an offset of about 100 micrometer or about 60% of the average grain diameter of the sample (Fig. 9e). The maps of marker particle trajectories in Figs. 9(d) and 9(f) indicate that this grain boundary sliding results mainly from a translation jump between grains 11 and 22.

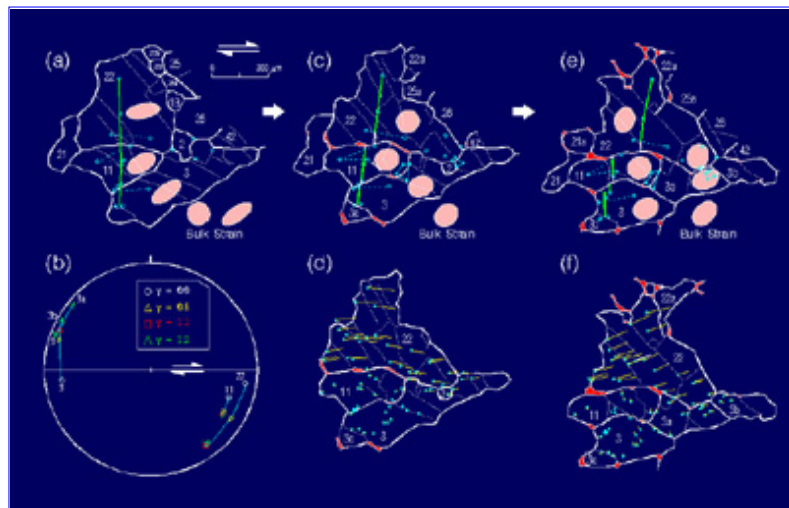


Fig. 9. (a) Map of some grains in sample TO-105. Strains represented by ellipses are strains accumulated from the beginning. Thick line (light green) is a material line. Dotted lines (white) are subgrain boundaries. Bulk strain ellipse represents a strain for the total area of the grains shown. Not all marker particles (light blue, small circle) used to calculate strains are shown. (b) c-axis trajectories of grains 3, 11 and 22. Grain 3 is recrystallized into three smaller grains later. Shear strains in the inset represent a bulk shear strain of the whole sample. Triangle, square and the tip of arrow correspond to stages (a), (c) and (e), respectively. (c) Offset of the material line by grain boundary sliding. Strain ellipses represent additional strain from (a). Areas outlined by four marker particles at the boundaries between grain 3 and 11, and adjacent to the junction among grains 2, 3, and 22, are indicated by light-blue lines. Grain boundary openings are in red. (d) Displacements of marker particles which remain in the same grain, relative to a fixed marker particle in grain 11 (solid circle) and the bulk shear direction horizontal. Open circles (light blue) are positions of marker particles at stage (a) and the other end of strokes (yellow) are positions at stage (c) or present positions. Solid circle (light blue) in grain 11 represents the fixed marker particle. (e) Further offset of the marker line. Strain ellipses represent additional strains from (a). (f) Displacements of marker particles from stage (c) to (e).

Across the grain boundaries under possible compression due to the grain boundary sliding, such as the boundary between grains 11 and 3a, and the boundary adjacent to the junction of grains 3a, 3b and 22 (Fig. 9e), the areas occupied by each four marker particles show only a few percent decrease from the stage of Fig. 9(c) to Fig. 9(e). This implies that diffusional accommodation is not significant at these sites. Note also that the grains are not perfectly rigid but are internally strained during grain boundary sliding. Grain 3 is more strongly strained than the other grains and shows rotational recrystallization resulting in grain-size reduction. This suggests that grain boundary sliding is accommodated mainly by intragranular plastic deformation at these compressional areas. At boundaries possibly under extension, grain boundary sliding causes openings to occur that could serve as sink sites of diffusion. Indeed, some grains show overgrowths into the grain boundary openings, suggesting diffusional influx into these sites (Fig. 7 and also see figs. 7e and f of Ree, 1994). The source sites of diffusion are not clear given the marker particle population and scale.

4.5. Grain Boundary Sliding by Rotation Jump and Accommodation by Grain Boundary Opening (TO-105)

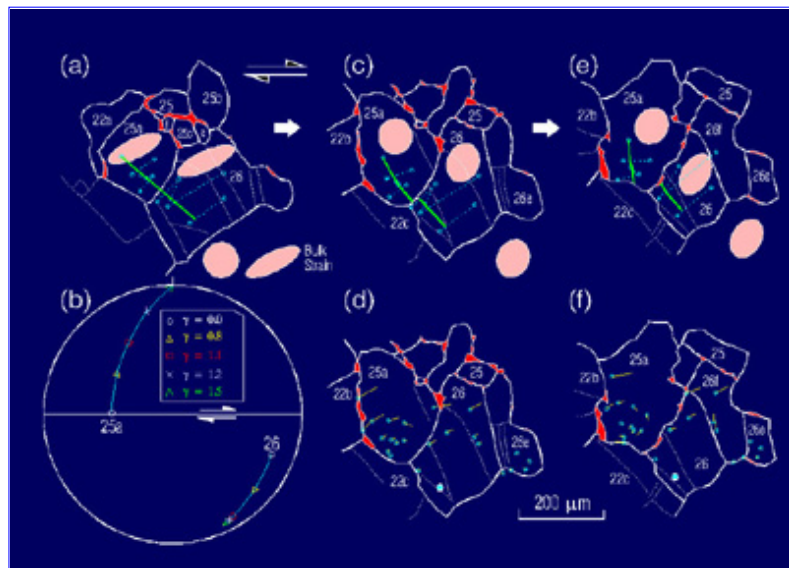


Fig. 10. Offset of a marker line (thick and green) crossing the boundary between grains 25a and 26 in sample TO-105 (a, c, & e). Ellipses in (a) indicate strains accumulated from the beginning of deformation. Bulk strain is the strain of the area around grains 25a and 26. Ellipses in (c) & (e) represent additional strains accumulated from (a). (b) c-axis trajectories of grains 25a and 26. Shear strains in the inset represents the bulk shear strain of the whole sample. The cross and tip of arrows indicate c-axis at stages (a) and (e), respectively. (d) Displacements of marker particles remaining in the same grain from (a) to (c) relative to a fixed marker particle in grain 26 (light-blue, solid circle) and the bulk shear direction horizontal. (f) Displacements of marker particles from (c) to (e).

Figure 10 shows grain boundary sliding due to a rotation jump between grains 25a and 26 in sample TO-105. As the sample is deformed, intragranular plastic deformation and clockwise c-axis rotation are followed by the formation of grain boundary openings, as in the previous example. After a bulk shear strain of about 1.2 (Fig. 10a), the two grains deform in significantly different manners. The trajectories of marker particles within grain 25a (Figs. 10d and f) and very weak intragranular deformation implied by the incremental, intragranular strain ellipses (Figs. 10c and e) indicate that grain 25a is deformed mainly by clockwise rigid-body rotation. The c-axis of grain 25a also rotates clockwise by about 20° (Fig. 10b), and its grain-size increases with the consumption of adjacent grains during this deformation interval. In contrast, the intragranular strain of grain 26 is stronger even than the bulk strain of the local area comprising these two grains. Grain 26 also shows grain-size reduction by rotational recrystallization and grain boundary migration (Figs. 10a, b, and c), and only a small rotation of its c-axis (Fig. 10b). Grain boundary sliding associated with the more or less rigid-body rotation of grain 25a is evidenced by the offset of a marker line drawn almost perpendicular to the boundary between the two grains. The healing and shape change of openings at the NE and SW boundaries of grain 25a, and the creation of openings at the boundary between grains 25a and 26, are associated with this grain boundary sliding (Fig. 10e). The reason why the two grains behave differently, even though the orientations of their c-axes relative to the shear direction are similar at the beginning of the deformation interval described above, is unclear. Perhaps the stress field is highly heterogeneous in that area.

4.6. Grain Boundary Sliding by Translation Jump and Accommodation by Diffusion and Grain Boundary Opening (TO-202)

Experiment TO-202 is the slowest simple shearing experiment described here (Table 1). The c-axis fabric diagram before deformation shows a broad girdle normal to the direction of shear as usually observed in other simple shearing experiments (Fig. 11f).

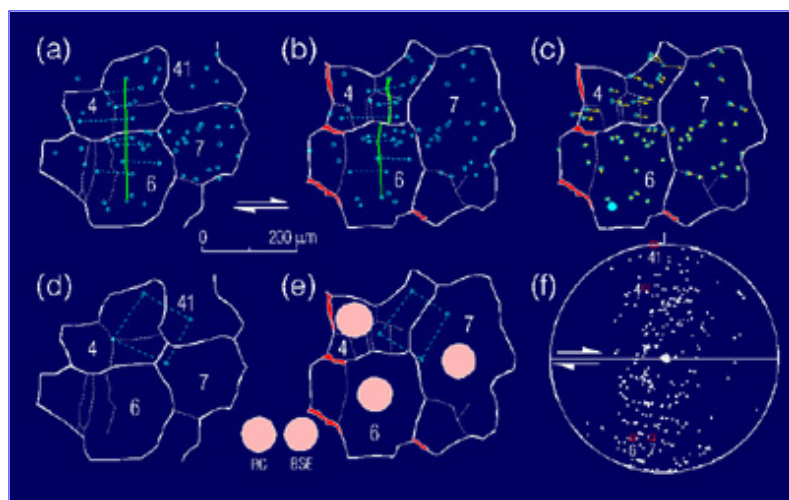


Fig. 11. (a) & (b) Offset of a marker line (thick, light green) crossing the boundary between grains 4 and 6 in sample TO-202. (c) Displacements (yellow) of marker particles (light blue) remaining in the same grain from (a) to (b), relative to a fixed marker particle in grain 6 (light-blue, solid circle). The bulk shear direction is horizontal. Duration of deformation in (a) & (b) is 19 and 27 hrs, respectively. (d) & (e) Change of an area outlined by four marker particles from (a) to (b). Ellipses in (e) indicate strains accumulated from (d). RC: reference circle for strain ellipse. BSE: Bulk strain ellipse of the local area around grains 4, 6 and 7. (f) c-axis fabric diagram before deformation. c-axes of grains shown in Figs. (a), (b) & (c) are numbered and marked as squares (red). Lower-hemisphere equal area projection.

As in experiment TO-105, extensive grain boundary openings associated with grain boundary sliding develop. They develop, however, at a lower shear strain than in TO-105 (less than 0.1). Their ratio is about 1 % of the sample area at shear strain of 0.1. Offset of a marker particle line and marker particle trajectories in Fig. 11 indicate that a translation jump is mainly responsible for the grain boundary sliding between grains 4 and 6 (Figs. 11a, b and c). Across a boundary which is possibly under compression due to the grain boundary sliding, the area occupied by four marker particles decreases by about 15% during an increment of bulk shear strain less than 0.1 (Figs. 11d and e), suggesting the removal of material by diffusion. The upper segment of the boundary between grains 4 and 7 (41 in the earlier stage) moves toward the marker particles in grain 4 as well as toward those in grain 7 (41 in the earlier stage, Figs. 12a and b). This suggests material efflux from both grains along the boundary. The lower segment of the boundary moves toward the marker particles in grain 4 and away from those in grain 7. The distance of the boundary movement toward the marker particles in grain 4 is larger than that of the boundary movement away from the marker particles in grain 7 (Figs. 11a and b). This may indicate that material efflux from grain 4 occurs together with the conventional volume-conserving grain boundary migration for the lower segment of the boundary. At an extensional site (the left boundary of grain 4), a grain boundary opening develops by grain boundary sliding. Preservation of contact between grain 4 and the grain to its left (not shown) along the lower part of the boundary, however, implies that a translation of the grain on the left or diffusional influx may also be involved at this site.

[Previous Section](#) [Home](#) [Next Section](#)

5. Evolution and Implications of Grain Boundary Sliding

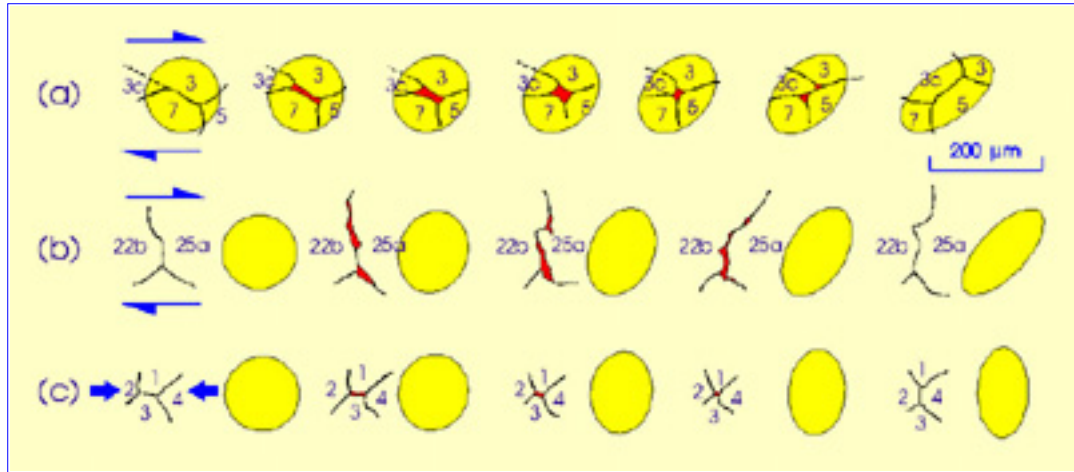


Fig. 12. Opening and closing of grain boundaries in simple shearing experiment TO-105 (a & b) and pure shearing experiment TO-100 (c). The bulk shear strains of the whole sample at the start of each sequence of (a) & (b) are about 1.0 and 1.3, respectively. In (c) the start of the sequence corresponds to the beginning of the deformation. Additional strains around grain boundaries or openings (red) are represented by strain ellipses (yellow).

The experimental examples show that openings grow preferentially along grain boundaries at low angles to the shortening direction with grain boundary sliding. Growth of openings usually involves four grains (Figs. 12a and c). Once openings grow, they are shortened parallel to the shortening direction by thrusting of sliding grains and grain overgrowth into the openings. With further deformation they are eventually closed leading to a neighbor switching of four grains (Figs. 12a and c). The magnitude of the minimum principal stretch associated with this neighbor switching is about 0.7. This value is somewhat larger than that (0.58) of Ashby and Verrall's (1973) neighbor switching model where coherency at the boundary is maintained by diffusion without opening. In some cases only two or three grains are involved in the opening and closing of a grain boundary without any neighbor switching (Fig. 12b). Here grain boundary openings are closed as one grain rigidly rotates and the grain boundary with openings becomes perpendicular to the shortening direction.

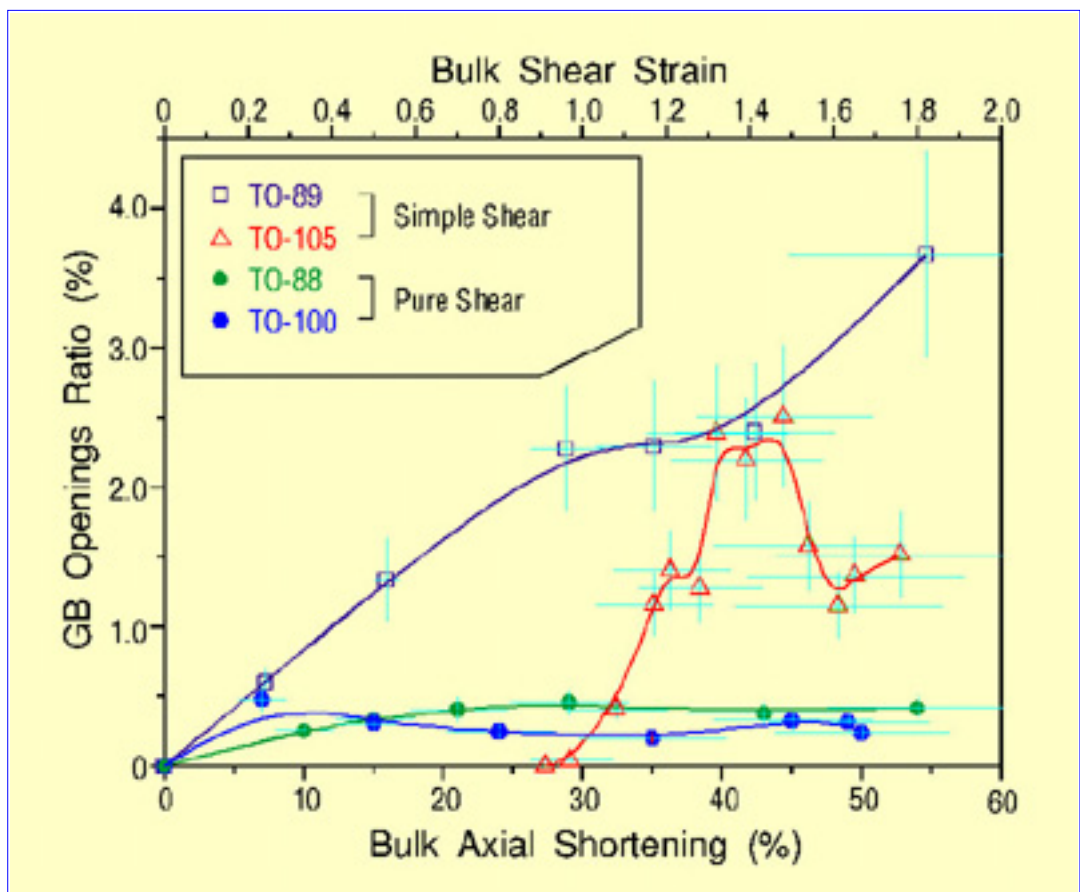
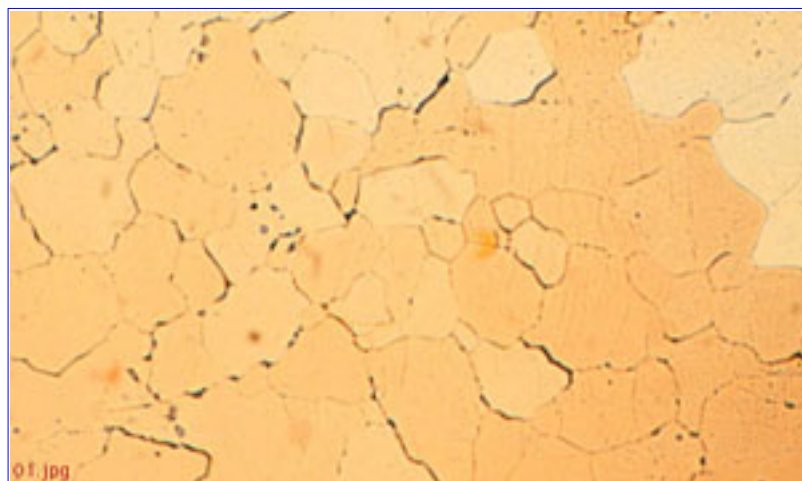


Fig. 13. Plot of bulk strain vs. grain boundary openings ratio. Horizontal bars (light blue) are 1 standard deviations of bulk strain. Vertical bars (light blue) are measurement error ranges of grain boundary openings ratio.

While grain boundary openings are being closed in some places, approximately the same area of grain boundary openings appear in other places, maintaining an approximately steady openings ratio of about 1 - 3% of the sample volume in these simple shearing experiments and of about 0.5% in pure shearing experiments without development of any large scale fracture (Figs. 7, 13 and 14). In one simple shearing experiment (TO-89), however, the ratio increases by a further 1% toward the end of the deformation. The mean residence time of individual openings corresponds to a shear strain increment of about 0.2 in experiment TO-105 (Ree, 1988). Almost all grain boundary openings disappear within 15-20 hours if the deformation is stopped but the temperature is maintained (Fig. 14).



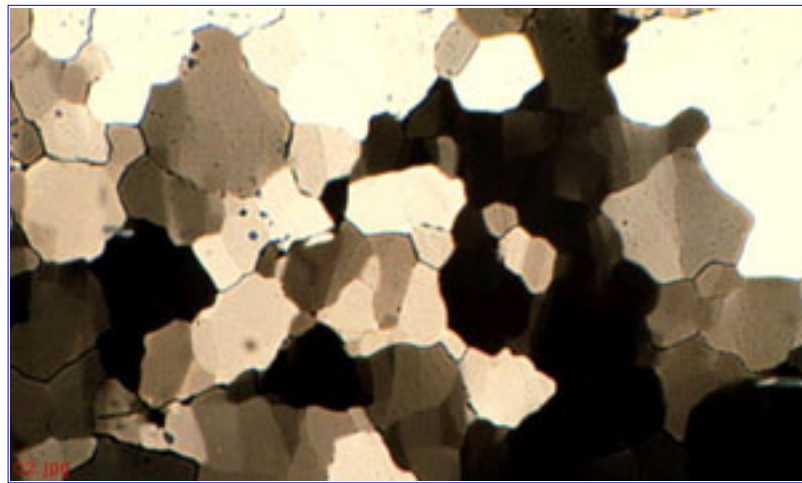


Fig. 14. Time-lapse movies of the deformation of sample TO-89 with plane light (a) and crossed-polars (b). The total shear strain = 1.8. The last frame of each movie shows the same field area after 16-h static heating. Note that all grain boundary openings disappeared with the static heating. Dextral shear direction is horizontal. Field width of each frame = 1.55 mm.

In Fig. 15, the orientations of grain boundary openings at the end of the deformation are shown as rose diagrams with the foliation orientation as a reference horizontal axis. The foliation orientation is defined statistically by the preferred orientation of long axes of grains in this paper. In experiments TO-89 (simple shearing experiment) and TO-88 (pure shearing experiment) the openings are preferentially oriented at a high angle to the foliation orientation. Their orientation is also symmetric with respect to the foliation orientation (Figs. 15a and c). In experiment TO-105, however, the preferred orientation of the grain boundary openings is at a low angle to the foliation orientation (Fig. 15b). However in this experiment, the average ratio of long axes to short axes of grains is very low (about 1.05). With this low value of average grain axial ratio, the definition of foliation orientation is of uncertain significance. In all experiments, the preferred orientation of grain boundary openings is at a high angle to the direction of the maximum finite stretch, and at a low angle to the shortening direction (Fig. 15). The orientations of grain boundary openings were also measured at several stages during deformation. They all show more or less constant distribution with respect to the shortening direction as in Fig. 15.

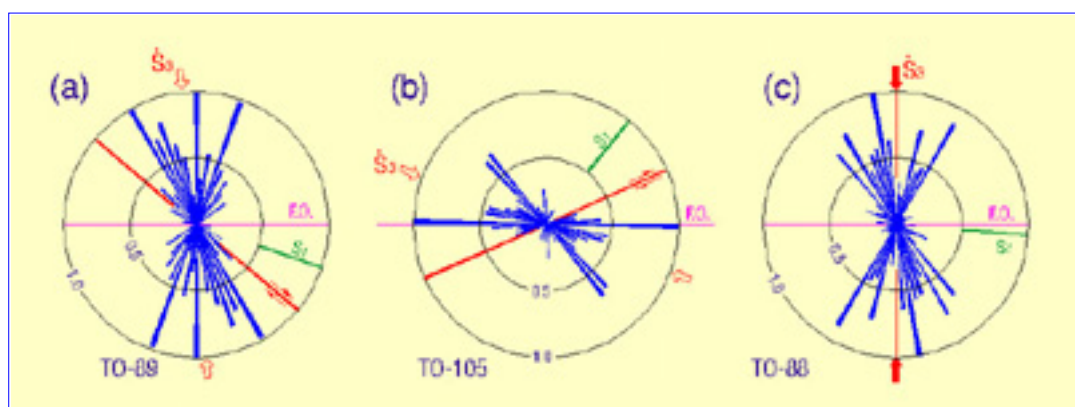


Fig. 15. Rose diagrams of grain boundary openings representing the total length of the long axis per angle of orientation in samples (a) TO-89, (b) TO-105 and (c) TO-88. The length of each orientation (5° interval) is normalized to the maximum length. FO: foliation orientation. S_1 : maximum finite stretch direction. S_3 : Shortening direction.

These grain boundary openings are strongly coupled with grain boundary sliding as explained earlier, and they can also significantly enhance diffusion by providing paths for rapid transport of matter through fluids filling the openings (White and White, 1981; Raj, 1982). In

natural conditions, fluid will probably circulate preferentially toward growing grain boundary openings and away from closing grain boundary openings. This circulating fluid will shift the sites at which reaction and alteration are concentrated, and will redistribute chemical components (Cox and Etheridge, 1989; McCaig and Knipe, 1990). More importantly, the creation of grain boundary openings dramatically increases the area through which diffusion can take place, thus enhancing the rate of diffusional transport.

The preferred alignment of grain boundary openings at low angles to the main shortening direction both in pure and simple shearing deformation (Fig. 15) suggests that it may be used as an indicator of the instantaneous stretching or flow stress orientation in situations where older, rotated openings are continuously removed.

The ratio of grain boundary openings is lower in pure shearing deformation than in simple shearing deformation (Fig. 13). This difference may result from the deformation configuration of the present apparatus where a thin sheet of OCP is deformed between two glass slides (see Means, 1989, fig. 1c and d). In simple shearing configuration there exists a tension along the stretching direction whereas there is no tension, only a weaker compression, along the stretching direction in pure shearing deformation. The presence of tension in the simple shearing experiments probably facilitates the development of grain boundary openings.

[Previous Section](#) [Home](#) [Next Section](#)

6. Recognition of Grain Boundary Sliding

White (1977) suggests several potential indicators of grain boundary sliding. These are: constant small grain size, equidimensional grain shape, random lattice orientation, bimodal alignment of grain boundaries, presence of grain boundary bubbles, and presence of high dislocation density adjacent to grain boundary irregularities and triple points. In addition to these, Beere (1978) and Fliervoet et al. (1997) showed that with a dominant grain boundary sliding, there is no crystallographic relation between adjacent grains due to grain rotation. Since the present technique of the experiment described in this paper does not allow the analysis of the microstructure on TEM/SEM scale, the last two indicators will not be discussed here.

In experiment TO-105, the average grain area at the end of the deformation is about $1.76 \times 10^{-2} \text{ mm}^2$, which is larger than that of experiment TO-110 (about $1.23 \times 10^{-2} \text{ mm}^2$). Since the grain boundary sliding is more extensive in experiment TO-105, smaller grain size does not necessarily favor grain boundary sliding.

In all experiments where grain boundary sliding appears to be extensive with the development of grain boundary openings, the average grain axial ratio is less than 1.4 throughout the deformation. This value is not much lower than that of experiment TO-110 (about 1.5 from shear strain = 0.9 onwards) where intragranular plastic deformation is more important. Also in another experiment, not described here (experiment TO-109), the average grain axial ratio is lower throughout the deformation (1.1 - 1.3) and intragranular plastic deformation is predominant. Therefore equidimensional grain shape may not be a good indicator of grain boundary sliding, particularly if grain-shape adjustment by grain boundary migration is effective (Rubie, 1990).

Random lattice orientation may not be a reliable indicator of grain boundary sliding either since sample TO-105 shows a strong lattice preferred orientation (Fig. 8). It has been suggested that some lattice preferred orientation could develop when grain boundary sliding is accommodated by intracrystalline slip (Edington et al., 1976; Etheridge and Wilkie, 1979; Schmid et al., 1987). Furthermore, Rutter et al. (1994) showed that in a deformation with dominant grain boundary sliding, there is only a weak development of lattice preferred orientation at 50% strain of fine-grained calcite aggregates, whereas there is a strong lattice preferred orientation at more than 600% strain, similar to that of intracrystalline plastic flow regime.

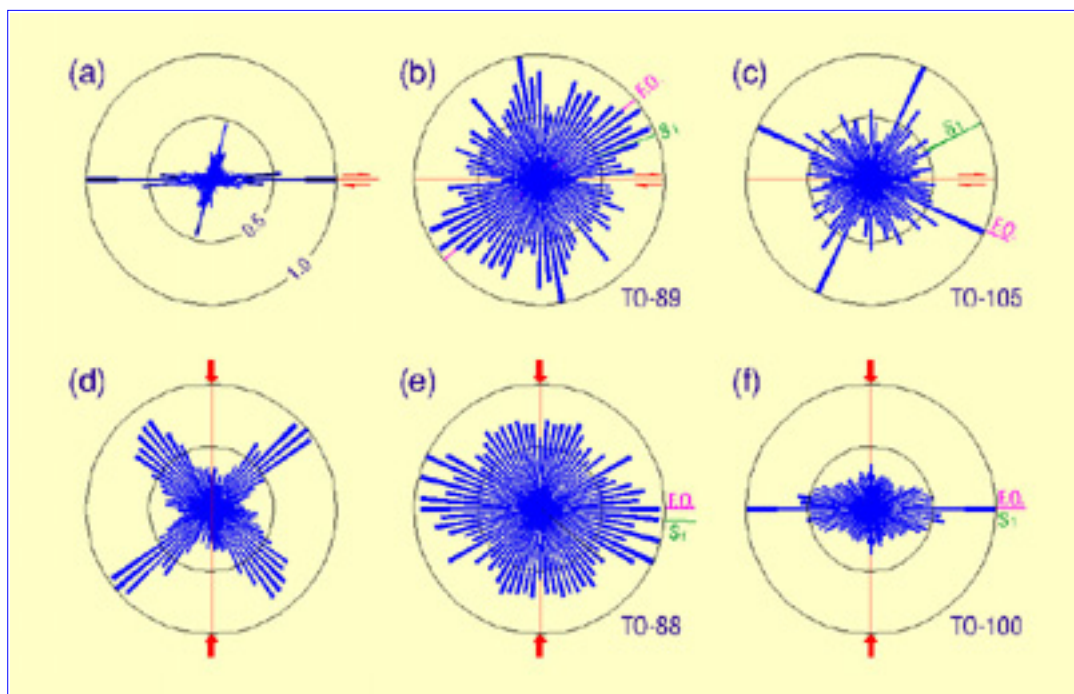


Fig. 16. Rose diagrams of grain boundaries representing the total length of grain boundaries per angle of orientation. (a) & (d) Grain boundary orientations measured from fig. 3 of Drury and Humphreys (1988). (b) & (c) Simple shearing experiment. (e) & (f) Pure shearing experiment. FO: foliation orientation. S_1 : maximum finite stretch direction.

Bimodal alignment of grain boundaries has been considered as a strong evidence of grain boundary sliding (Raj and Ashby, 1971; Singh et al., 1973; White, 1977; Schmid et al., 1987; Drury and Humphreys, 1988). In simple shear deformation the first maximum is known to be parallel to the shear zone boundary with the second maximum being at about 70° to the shear zone boundary (Fig. 16a, Schmid et al., 1987; Drury and Humphreys, 1988). In pure shear deformation, two maxima are known to be symmetric with respect to the shortening direction with an angle of about 45° (Fig. 16d, Singh et al., 1973; White, 1977; Drury and Humphreys, 1988). Although the grain boundary orientation in experiment TO-105 shows two maxima perpendicular to each other, with one maximum 25° off from the bulk shear direction (Fig. 16c), other experiments do not generate a preferred bimodal alignment of grain boundaries (Figs. 16b, e and f).

The preferred orientation of grain boundary openings is seen to be a reliable criterion of grain boundary sliding in experiments described here (Fig. 15). The disappearance of grain boundary openings during static readjustment of the microstructure after deformation (Fig. 14) suggests that it may not be a valuable indicator of grain boundary sliding in naturally deformed rocks. However, if grain boundaries are found to carry remnants of former grain boundary openings such as an array of bubbles or voids and of second phase inclusions in observation under electron microscopy (White and White, 1981; Behrmann, 1985; Fliervoet et al., 1997), and if these grain boundaries have a well-defined preferred orientation (Behrmann and Mainprice, 1987), these will be a strong indicator of the former existence of grain boundary openings and grain boundary sliding. Preferred orientation of grain boundary bands with a slightly different chemical composition from the grain interior (Hall, 1984) might be another possible indicator of grain boundary opening and sliding.

In summary, any single indicator alone of all above, except preferred orientation of remnants of grain boundary openings, does not satisfactorily imply grain boundary sliding. The main reason for this is probably that accommodation mechanisms for grain boundary sliding will

easily erase the signatures of grain boundary sliding.

Acknowledgements

I thank my teacher, Prof. W.D. Means, for his continuous support and patience while I was at Albany. I also thank Youngdo Park for his help with making movies used in this paper. The manuscript was improved by comments from Paul Bons and Mark Jessell. The publication of this paper was partially supported by Korea Science and Engineering Foundation grant 981-0401-005-2.

[Previous Section](#) [Home](#) [Next Section](#)

7. References

- Adams, M. A. and Murray, G. T. (1962) Direct observations of grain boundary sliding in bi-crystals of sodium chloride and magnesia. *J. appl. Phys.* **33**, 2126-2131.
- Ashby, M. F. and Verrall, R. A. (1973) Diffusion-accommodated flow and superplasticity. *Acta metall.* **21**, 149-163.
- Beere, W. (1978) Stresses and deformation at grain boundaries. *Phil. Trans. R. Soc. Lond.* **A288**, 177-196.
- Behrmann, J. H. (1985) Crystal plasticity and superplasticity in quartzite; a natural example. *Tectonophysics* **115**, 101-129.
- Behrmann, J. H. and Mainprice, D. (1987) Deformation mechanisms in a high-temperature quartz-feldspar mylonite: evidence for superplastic flow in the lower continental crust. *Tectonophysics* **140**, 297-305.
- Bons, P. D. and Urai, J. L. (1992) Syndeformational grain growth: microstructures and kinetics. *J. Struct. Geol.* **14**, 1101-1109.
- Chokshi, A. H. and Langdon, T. G. (1985) The role of interfaces in superplastic deformation. In *Superplasticity*, eds B. Baudelet and M. Suery, pp. 1-15. Centre Nationale de la Recherche Scientifique **2**.
- Chokshi, A. H. and Langdon, T. G. (1987) A model for diffusional cavity growth in superplasticity. *Acta metall.* **35**, 1089-1101.
- Cox, S. F. and Etheridge, M. A. (1989) Coupled grain-scale dilatancy and mass transfer during deformation. *J. Struct. Geol.* **11**, 142-162.
- Crossman, F. W. and Ashby, M. F. (1975) The non-uniform flow of polycrystals by grain-boundary sliding accommodated by power law creep. *Acta metall.* **23**, 425-440.
- Drury, M. R. and Humphreys, F. J. (1986) The development of microstructure in Al5%Mg during high temperature deformation. *Acta metall.* **34**, 2259-2271.
- Drury, M. R. and Humphreys, F. J. (1988) Microstructural shear criteria associated with grain boundary sliding during ductile deformation. *J. Struct. Geol.* **10**, 83-89.
- Drury, M. R. and Urai, J. L. (1990) Deformation-related recrystallization processes. *Tectonophysics* **172**, 235-253.
- Edington, J. W., Melton, K. N. and Cutler, C. P. (1976) Superplasticity. *Prog. Mater. Sci.* **21**, 63-170.
- Edward, G. H. and Ashby, M. F. (1979) Intergranular fracture during power-law creep. *Acta metall.* **27**, 1505-1518.
- Etheridge, M. A. and Wilkie, J. C. (1979) Grain size reduction, grain boundary sliding and the flow strength of mylonites. *Tectonophysics* **58**, 159-178.
- Fliervoet, T. F., White, S. H. and Drury, M. R. (1997) Evidence for dominant grain-boundary sliding deformation in greenschist- and amphibolite-grade polymineralic ultramylonites from

the Redbank Deformed Zone, Central Australia. *J. Struct. Geol.* **19**, 1495-1520.

Gifkins, R. C. (1976) Grain-boundary sliding and its accommodation during creep and superplasticity. *Met. Trans.* **7A**, 1225-1232.

Gilotti, J. A. and Hull, J. M. (1990) Phenomenological superplasticity in rocks. In *Deformation Mechanisms, Rheology and Tectonics*, eds R. J. Knipe and E. H. Rutter, pp. 229-240. Geological Society Special Publication **54**.

Hall, P. C. (1984) Some aspects of deformation fabrics along the Highland/Lowland boundary, northwest Adirondacks, New York State. Unpublished M. S. thesis, State University of New York at Albany.

Hashimoto, S., Fujii, T. K. and Miura, S. (1987) Grain-boundary sliding and triple-point fold in aluminum tricrystals. *Scr. Met.* **21**, 169-174.

Kashyap, B. P., Arieli, A. and Mukherjee, A. K. (1985) Review: microstructural aspects of superplasticity. *J. Mat. Sci.* **20**, 2661-2686.

Knipe, R. J. (1989) Deformation mechanisms - recognition from natural tectonites. *J. Struct. Geol.* **11**, 127-146.

Langdon, T. G. (1970) Grain boundary sliding as a deformation mechanism during creep. *Phil. Mag.* **22**, 689-700.

Langdon, T. G. (1975) Grain boundary deformation processes. In *Deformation of Ceramic Materials*, eds R. C. Bradt and R. E. Tressler, pp. 101-126. Plenum, New York.

Langdon, T. G. (1981) Deformation of polycrystalline materials at high temperatures. In *Deformation of Polycrystals: Mechanisms and Microstructures*, eds N. Hansen, A. Horsewell, T. Leffers and H. Lilholt, pp. 45-54. Riso Nat. Lab., Roskilde, Denmark.

Langdon, T. G. and Vastava, R. B. (1982) An evaluation of deformation models for grain boundary sliding. In *Mechanical Testing for Deformation Model Development*, eds R. W. Rohde and J. C. Swearingen, pp. 435-451. American Society for Testing materials, Philadelphia.

Marya, S. K. and Wyon, G. (1975) Superplasticite a l'ambiente de l'aluminium a grain fin, en liaison avec l'existence d'un film intergranulaire de solution solide riche en gallium. *J. Physique* **36**, C.4, 309-313.

Mainprice, D. H. and Paterson, M. S. (1984) Experimental studies of the role of water in the plasticity of quartzite. *J. geophys. Res.* **89**, 4257-4296.

McCaig, A. M. and Knipe, R. J. (1990) Mass-transport mechanism in deforming rocks: recognition using microstructural and microchemical data. *Geology* **18**, 824-827.

Means, W. D. (1989) Synkinematic microscopy of transparent polycrystals. *J. Struct. Geol.* **11**, 163-174.

Means, W. D. and Jessell, M. W. (1986) Accommodation migration of grain boundaries. *Tectonophysics* **127**, 67-86.

Means, W. D. and Ree, J.-H. (1990) Structural motion, particle motion, and migration processes in deforming materials. *Geol. Soc. Am. Abs. w. Prog.* **22**, A138.

- Mitra, S. (1976) A quantitative study of deformation mechanisms and finite strain in quartzites. *Contr. Miner. Petrol.* **59**, 203-226.
- Naziri, H., Pearce, R., Henderson-Brown, M. and Hale, K. F. (1973) In situ superplasticity experiment in the 1 million volt electron microscope. *J. Microscopy* **97**, 229-238.
- Naziri, H., Pearce, R., Henderson-Brown, M. and Hale, K. F. (1975) Microstructural-mechanism relationship in the zinc-aluminum eutectoid superplastic alloy. *Acta metall.* **23**, 489-496.
- Paquet, J. and Francois, P. (1980) Experimental deformation of partially melted granitic rock at 600 - 900° C and 250MPa confining pressure. *Tectonophysics* **68**, 131-146.
- Peach, C. J. and Spiers, C. J. (1996) Influence of crystal plastic deformation on dilatancy and permeability development in synthetic salt rock. *Tectonophysics* **256**, 101-128.
- Poirier, J. P. (1985) *Creep of Crystals*. Cambridge University Press, Cambridge.
- Raj, R. (1982) Creep in polycrystalline aggregates by matter transport through a liquid phase. *J. geophys. Res.* **87**, 4731-4739.
- Raj, R. and Ashby, M. F. (1971) On grain boundary sliding and diffusional creep. *Met. Trans.* **2**, 1113-1127.
- Ree, J.-H. (1988) Evolution of deformation-induced grain boundary voids in octachloropropane. *Geol. Soc. Am. Abs. w. Prog.* **20**, A213.
- Ree, J.-H. (1990) High temperature deformation of octachloropropane: dynamic grain growth and lattice reorientation. In *Deformation Mechanisms, Rheology and Tectonics*, eds R. J. Knipe and E. H. Rutter, pp. 363-368. Geological Society Special Publication **54**.
- Ree, J.-H. (1991) An experimental steady-state foliation. *J. Struct. Geol.* **13**, 1001-1011.
- Ree, J.-H. (1994) Grain boundary sliding and development of grain boundary openings in experimentally deformed octachloropropane. *J. Struct. Geol.* **16**, 403-418.
- Rubie, D. C. (1990) Mechanisms of reaction-enhanced deformability in minerals and rocks. In *Deformation Processes in Minerals, Ceramics and Rocks*, eds D. J. Barber and P. G. Meredith, pp. 262-295. Unwin Hyman, London.
- Rutter, E. H., Casey, M. and Burlini, L. (1994) Preferred crystallographic orientation development during the plastic and superplastic flow of calcite rocks. *J. Struct. Geol.* **16**, 1431-1446.
- Schmid, S. M. (1982) Microfabric studies as indicators of deformation mechanisms and flow laws operative in mountain building. In *Mountain Building Processes*, ed K. J. Hsü, pp. 95-110. Academic Press, London.
- Schmid, S. M., Boland, J. N. and Paterson, M. S. (1977) Superplastic flow in fine-grained limestone. *Tectonophysics* **43**, 257-291.
- Schmid, S. M., Panozzo, R. and Bauer, S. (1987) Simple shear experiments on calcite rocks: rheology and microfabric. *J. Struct. Geol.* **9**, 747-778.
- Singh, V. Rao, P. and Taplin, D. M. R. (1973) On the role of grain boundary migration during

the creep of zinc. *J. Mater. Sci.* **8**, 373-381.

Speight, M. V. (1976) The role of grain-boundary sliding in the creep of polycrystals. *Acta metall.* **24**, 725-729.

Stowell, M. J., Livesey, D. W. and Ridley, N. (1984) Cavity coalescence in superplastic deformation. *Acta metall.* **32**, 35-42.

Stünitz and Fitz Gerald, (1993) Deformation of granitoids at low metamorphic grade II: Granular flow in albite-rich mylonites. *Tectonophysics* **221**, 299-324.

Urai, J. L., Means, W. D. and Lister, G. S. (1986) Dynamic recrystallization of minerals. In *Mineral and Rock Deformation: Laboratory Studies-The Paterson Volume* eds H. C. Heard and B. E. Hobbs, pp. 161-199. *Am. Geophys. Un. Geophys. Monogr.* **36**.

Vastava, R. B. and Langdon, T. G. (1979) An investigation of intercrystalline and interphase boundary sliding in the superplastic Pb-62% Sn eutectic. *Acta metall.* **27**, 251-257.

Weber, K. (1986) Metamorphism and crustal rheology - implications for the structural development of the continental crust during prograde metamorphism. In *The Nature of the Lower Continental Crust*, eds J. B. Dawson, D. A. Carswell, J. Hall and K. H. Wedepohl, pp. 95-106. Geological Society Special Publication **24**.

White, J. C. and White, S. H. (1981) On the structure of grain boundaries in tectonites. *Tectonophysics* **78**, 613-628.

White, S. (1977) Geological significance of recovery and recrystallization processes in quartz. *Tectonophysics* **39**, 143-170.

Zeuch, D. H. (1984) Application of a model for grain boundary sliding to high temperature flow of Carrara Marble. *Mechanics of Materials* **3**, 111-117.

Zhang, Y., Hobbs, B. E. and Jessell, M. W. (1994) The effect of grain-boundary sliding on fabric development in polycrystalline aggregates. *J. Struct. Geol.* **16**, 1315-1325.

[Previous Section](#) [Home](#) [Next Section](#)